ΠΑΝΕΠΙΣΤΗΜΙΟ ΠΑΤΡΩΝ
UNIVERSITY OF PATRAS

THESIS

Probing fundamental physics using compact objects

Kolonia Eleni Anna

Supervisors:

Martins, C.J.A.P.
Researcher, Center of Astrophysics,
University of Porto (CAUP)

Gourgouliatos, Konstantinos
Associate Professor, Department of Physics,
University of Patras

Patras 2024

This work has been carried out in the context of the activities of the Theoretical Astrophysics research group at the Department of Physics of the University of Patras, as well as the Phi in the Sky research group of the Center of Astrophysics of the University of Porto.

http://www.astro.upatras.gr/el/astrotheory

Abstract

It is well known that alternative theories to the Standard Model allow fundamental constants, such as the fine structure constant, to vary in spacetime. One way to investigate these variations is to utilize the Mass-Radius relation of compact objects, which is inherently affected by α variations. As such, we initially construct the model of a polytropic white dwarf, which we perturb by adding the α variations for various GUT models. We continue our analysis with neutron stars, investigating both polytropic and more realistic equations of state. We outline how future observations might distinguish between extensions of the Standard Model.

Περίληψη

Είναι ευρέως γνωστό ότι τα Καθιερωμένα Πρότυπα τόσο της Κοσμολογίας, όσο και της Σωματιδιακής Φυσικής αδυνατούν να εξηγήσουν πλήρως μέχρι τώρα κάποια παρατηρούμενα φαινόμενα. Έτσι, η επιστημονική κοινότητα καταφεύγει σε επεκτάσεις τους ή ακόμα και εναλλακτικές θεωρίες για να τα εξηγήσει. Από την πλευρά της Κοσμολογίας, η χρήση βαθμωτών πεδίων (scalar fields) συνεισφέρει σημαντικά στην ερμηνεία του Πληθωρισμού, ενώ οδήγησε ήδη την προηγούμενη δεκαετία στην ανακάλυψη του μποζονίου Higgs. Αναπόφευκτη συνέπειά τους είναι παράλληλα η εμφάνιση χωροχρονικών και τοπικών διακυμάνσεων των θεμελιωδών σταθερών. Στην παρούσα διατριβή, επικεντρωνόμαστε στη σταθερά λεπτής υφής α, η οποία αποτελεί μέτρο της ισχύος της ηλεκτρασθενούς αλληλεπίδρασης.

Έχοντας αποδειξεί πειραματικά ότι η ισχύς των θεμελιωδών αλληλεπιδράσεων μεταβάλλεται με την ενέργεια, ερευνητές καταφεύγουν σε μια νέα ομάδα θεωριών, τις Μεγαλοενοποιημένες Θεωρίες, οι οποίες υποστηρίζουν την ενοποίηση των ισχυρών με τις ηλεκτρασθενείς αλληλεπιδράσεις στις υψηλές ενέργειες. Θα μελετήσουμε 3 τέτοια παραδείγματα θεωριών που καλύπτουν μεγάλο εύρος του παραμετρικού χώρου αυτών των μοντέλων.

Από την άλλη έχουμε αστρικά πτώματα όπως λευκοί νάνοι και αστέρες νετρονίων που αποτελούν σημαντικά εργαστήρια και πηγές δεδομένων για τους ερευνητές, λόγω των ακραίων συνθηκών που τους χαρακτηρίζει. Οι πρώτοι αποτελούνται από άνθρακα και οξυγόνο συμπιεσμένο σε πυκνοτητες πολύ μεγαλύτερες από τους συνήθεις αστέρες. Παράλληλα, οι πιέσεις που επικρατούν στους αστέρες νετρονίων αναγκάζουν τις πυρηνικές δομές να διαλυθούν, δημιουργώντας μια θάλασσα από νετρόνια, πρωτόνια και ηλεκτρόνια. Η δυναμική τέτοιων αστέρων περιγράφεται από τις εξισώσεις Tolman-Oppenheimer-Volkov (TOV) σε συνδυασμό με μία καταστατική εξίσωση. Ίσως το σημαντικότερο παρατηρούμενο χαρακτηριστικό τους είναι η σχέση Μάζας-Ακτίνας, η οποία επηρεάζεται σε μεγάλο βαθμό από διακυμάνσεις της σταθεράς λεπτής υφής και των Μεγαλοενοποιημένων Θεωριών. Συνεπώς αποτελεί ιδανικό εργαλείο για τους σκοπούς της παρούσας έρευνας.

Μπορούμε να μοντελοποιήσουμε έναν πολυτροπικό λευκό νάνο στα πλαίσια Μεγαλοενοποιημένων Θεωριών (με την προσθήκη βαθμωτού πεδίου που επιτρέπει χωροχρονική διακύμανση του α), διαταρράσσοντας τις εξισώσεις TOV στο σχετικιστικό και μη σχετικιστικό όριο. Αυτό

μας το επιτρέπει η καταστατική εξίσωση (πολυτροπική), η οποία έχει αναλυτική μορφή. Στην περίπτωση που επιθυμούμε να επαναλάβουμε τη διαδικασία με καταστατική εξίσωση σε αριθμητική μορφή, όπως θα επιχειρήσουμε με αστέρες νετρονίων, το πρόβλημα γίνεται αδύνατο να επιλυθεί με την υπάρχουσα μεθοδολογία. Συνεπώς καταφεύγουμε σε προσεγγιστικές σχέσεις Μάζας-Ακτίνας και στην ανάπτυξη κώδικα στη γλώσσα Python, για να καταστεί δυνατή η αριθμητική επίλυση του προβλήματος.

Τα αποτελέσματα που λαμβάνουμε χαρακτηρίζονται από συνοχή, γεγονός που αποδεικνύει τη συστηματικότητα της μεθοδολογίας που ακολουθούμε. Παρόλα αυτά, υπάρχει αρκετός χώρος για βελτίωση και επέκταση της ανάλυσης μας σε άλλα μοντέλα καταστατικών εξισώσεων και ευρύτερο παραμετρικό χώρο όσον αφορά τις Μεγαλοενοποιημένες Θεωρίες.

Table of Contents

1 Symbols and formalism **8**

2 Introduction **9**

3 Unification and Varying couplings **11**

1. Scalar fields 11

2. Varying fundamental couplings and Interactions 12

3. Unification and Grand Unified Theories 14

4 Compact Objects **16**

1. Formation 16

2. Composition and equilibrium 17

3. The Polytrope 18

4. Observations and measurements 19

5 White Dwarfs **22**

1. Perturbations 22

2. Results 24

6 Neutron Stars I: Methodology **29**

1. Perturbations 29

2. Numerical EoS 30

7 Neutron Stars II: Results **35**

8 Conclusions **38**

A White Dwarf Code **42**

B Neutron Star Code **50**

1

Symbols and formalism

Symbol	Description	Value
α	Fine structure constant	
γ	Polytropic exponent	$1 + \frac{1}{n}$
ϵ	Energy density	
ρ	Matter density	
$(any\ quantity)_*$	Planck units	
c	Speed of light	$299792458\ ms^{-1}$
G	Gravitational constant	$6.6743 \times 10^{-11} m^3 kg^{-1} s^{-2}$
$\bar{h}$	Reduced Planck constant	$1.05457182 \times 10^{-34} m^2 kg s^{-1}$
$M(r)$	Mass enclosed within radius r	
m_e	Electron mass	$9.1093837 \times 10^{-31} kg$
m_n	Neutron mass	$1.674927471 \times 10^{-27} kg$
m_N	Nucleon mass	$\frac{m_p + m_n}{2}$
m_p	Proton mass	$1.67262192 \times 10^{-27} kg$
$M_{solar,sun,\odot}$	Solar Mass	$1.9891 \times 10^{30} kg$
p	Pressure	
R	Total radius of the star	

2

Introduction

The quest to understand the fundamental laws of physics has driven scientific inquiry for centuries. From the classical mechanics of Newton to the quantum mechanics and relativity of the 20th century, physicists have continually sought to unify and explain the forces governing the universe. One of the most ambitious goals in this attempt is the formulation of Grand Unified Theories (GUTs), which aim to merge the electromagnetic, weak, and strong nuclear forces into a single framework. Additionally, the investigation into the constancy of fundamental constants, such as the fine structure constant (α), forms a crucial part of this pursuit.

Compact objects such as white dwarfs and neutron stars serve as natural laboratories for probing these deep questions. These remnants of stellar evolution are characterized by extreme conditions of density, gravity, and magnetic fields, providing physicists with an excellent probe for testing theories not only in fundamental physics but also in astrophysics, cosmology, nuclear physics, magnetohydrodynamics, and solid-state physics.

Despite advances in theoretical physics, experimental verification of GUT predictions is still limited. This thesis aims to address this issue by utilizing the research capabilities that compact objects can offer within this context. Specifically, our main goals are:

- To determine how these fundamental theories combined with a variation of the fine structure constant affect the properties of compact objects.
- To test GUT models in the extremities of a compact object's interior

and attempt to constrain them.

In the following Chapters, we will begin our analysis by first explaining the theoretical background behind varying couplings and unification (Chapter 3), and the dynamics of compact objects (Chapter 4). Then, we will move on to investigate a toy model of a white dwarf (Chapter 5), to gain some intuition before we move on to a more realistic neutron star model (Chapters 6, 7).

3

Unification and Varying couplings

A wide and fast-growing range of observational data has so far validated the Standard Model of particle physics and that of cosmology (ΛCDM). Nevertheless, evidence for dark matter and other phenomena such as inflation, neutrino masses, and the size of the baryon asymmetry in the universe require new physics beyond the current model. This is a hot topic in both fields at the moment, with theorists striving to come up with extensions or even alternative models to the standard ones. Their main objective is to test fundamental laws and symmetries such as the Equivalence Principle and Lorentz invariance, to determine possible violations and inconsistencies. In search of a way to explain dark matter, dark energy, and other enigmas, novel particles, cosmological scalar fields, magnetic monopoles, and fundamental strings are also introduced.

1. Scalar fields

Scalar fields nowadays are considered an essential component of many theories, due to their simplicity combined with their effectiveness. They can preserve Lorentz invariance while simultaneously taking a vacuum expectation value, which is impossible for other fields such as vector fields or fermions. But probably the most important argument to take into account is the fact that they have been experimentally proven to exist. The discovery of the Higgs particle, a product of the Higgs scalar

field, in 2012 by the ATLAS and CMS experiments at the Large Hadron Collider (LHC) at CERN, significantly popularized their implementation in models. This discovery also proved that scalar fields can be relatively easy to trace using observations and experiments, compared to other degrees of freedom, since they imply the production of additional particles and measurable effects. Some notable examples of them include [1]:

- **Inflation**, which is believed to have created the primordial density fluctuations that we now observe as large-scale cosmic structures.
- **Cosmological phase transitions and their relics**, such as cosmic strings, magnetic monopoles, and domain walls
- An alternative to Einstein's cosmological constant Λ, known as **dynamical dark energy**
- **The space-time and local variation of nature's fundamental couplings**, which is an unavoidable result in many extensions of the Standard Model of particle physics when there is a scalar field coupled to it.

2. Varying fundamental couplings and Interactions

The last, but vastly important result of scalar fields will be the main topic of our analysis in the following chapters. It is commonly known that dimensionless couplings *run* with energy. A straightforward example of this behavior is the fine structure constant, whose low-energy limit is approximately $\alpha = \frac{1}{137}$, which in the relativistic limit equals $\frac{1}{127}$. This occurs due to vacuum polarization (QED), which suggests that the vacuum is not just empty space, but is filled with virtual particle-antiparticle pairs that form and annihilate. These pairs screen the charge of an electron, leading to a modification of the electromagnetic force at different distances. So in smaller distances (higher energies), the screening effect becomes less effective, causing the observed value of α to increase. In many extensions of the Standard Model, such couplings also *roll* in time and *ramble* in space. Measurements of these variations could potentially be used as probes for fundamental cosmology.

Interaction	Coupling	Strength	Relative Strength	Range
Strong	α_s	$\sim 10^{-1}$	10^{38}	10^{-15}
Electromagnetic	$\alpha_{em} = \alpha = \frac{e^2}{\hbar c}$	$\frac{1}{137}$	10^{36}	∞
Weak	α_w	$\sim 10^{-5}$	10^{33}	10^{-18}
Gravity	$\alpha_g = \frac{Gm_p^2}{\hbar c}$	$\sim 10^{-38}$	1	∞

3.1: Fundamental forces ranked by their strength relative to gravity. The electromagnetic coupling is the known fine structure constant and the mediator of the gravitational interaction is the hypothetical graviton.

As explained above, if a scalar field is coupled to the Lagrangian of the model, that results in varying couplings. In particular, if the field couples to the electromagnetic part of that Lagrangian for example, it induces a variation in α, formulated as such:

$$\frac{\Delta\alpha}{\alpha}(z) = \frac{\alpha(z) - \alpha_0}{\alpha_0} \tag{3.1}$$

with α_0 being the present-day value of α.

The objective of this thesis is to investigate spacetime variations of couplings related to fundamental forces. In our current understanding of the universe, there are 4 fundamental forces, namely: gravitational, electromagnetic, strong, and weak nuclear force. The first two are strongly evident in our everyday reality (Earth's gravitational field and electromagnetic radiation) while the rest are related to subatomic processes like nuclear stability and β decay. The way they couple to a particle changes depending on its properties but also the type of interaction involved. Consequently, every force has a distinct parameter indicating its strength, the coupling. This strength for every interaction can be seen in Table [3.1], relative to the gravitational force which is, by convention, set to unity.

Apart from variations with energy, which will be discussed below, spatial and local variations are also allowed when a scalar field is coupled to a Lagrangian. This can be demonstrated mathematically as well. The Lagrangian component for the scalar field is:

$$\mathcal{L}_\phi = \frac{1}{2}\dot{\phi}^2 - V(\phi) \tag{3.2}$$

As a result of the field's coupling to the Lagrangian, and due to the properties of scalar fields mentioned above (they have a vacuum value while conserving symmetry), the electromagnetic component for instance

will include an additional coefficient, dependent on ϕ:

$$\mathcal{L}_{em} = -\frac{1}{4} B_F(\phi) F_{\mu\nu} F^{\mu\nu}, \tag{3.3}$$

where $\frac{\Delta\alpha}{\alpha} = \frac{\alpha(\phi)}{\alpha_0} - 1 = 1 - \frac{1}{B_F(\phi)}$. The same occurs for the rest of the components in the Lagrangian. We note that the gauge kinetic term above can be linearized since changes to the standard behavior have to be small. In some cases the second term in the scalar field Lagrangian (eq.3.2) depends also on the matter density, leading to local variations of fundamental constants. As a result, massive objects such as stars or black holes significantly influence varying α, thus including dependencies on local conditions and complicating the model. For that reason, we only focus on energy and spacetime variations.

3. Unification and Grand Unified Theories

The main goal of theorists is to build a simple yet consistent model, that explains the Universe from the biggest scales to the smallest. In the past, all fundamental interactions were modeled by separate theories that couldn't be united, for example, General Relativity for gravity and Quantum Electrodynamics for electromagnetism. However, in 1979 Abdus Salam, Sheldon Glashow, and Steven Weinberg were awarded the Nobel Prize in Physics for proving the unification of electromagnetic and weak interaction at high energies. Later this was also demonstrated with experiments, thus cementing the validity of this new electroweak theory. We can visualize the above model using Figure 3.1. Since couplings run with energy, their inverse will resemble a line, that differs for every coupling. As a result at some energy value, at least two lines will merge and unify, forming a different line that resembles the unified interaction. In the case of electroweak force, we know the position of this unification point on the energy axis to be at 100 GeV. In Figure 3.1, this is the first point where the blue (α_w^{-1}) and pink (α_{em}^{-1}) lines merge into purple.

This was a big step for the scientific community, as our understanding of fundamental forces became simpler and more coherent. Inspired by this achievement, more theories emerged supporting the unification of gravity (quantum gravity) and the strong force (QCD) with the electroweak interaction. We will focus on the latter class of models, Grand Unified Theories. They claim, in a similar manner to the electroweak

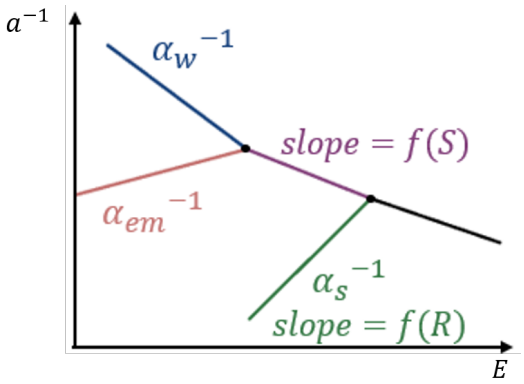

3.1: Qualitative plot of the inverse couplings as a function of energy. Note that the x-axis (E) is in logarithmic scale.

theory, that there must be some energy point, higher than electroweak unification, that the electroweak and QCD lines in Figure 3.1 merge to form a novel electronuclear interaction. Different GUTs assume different energies at which unification occurs and are parameterized by R and S, related to the energy scale at which unification is supposed to occur, which influences the slopes of the QCD and electroweak lines, respectively. These parameters consequently affect the slopes shown in Figure 3.1 and are typically positive. As a first test in our analysis, we will use 3 different GUTs that cover a representative portion of the (R, S) parametric space. These are the following:

- Unification scenario with $(R = 36, S = 160)$ [2]
- Dilaton scenario with $(R = 109.4, S = 0)$ [3]
- UV-Cutoff scenario with $(R = -183, S = 22.5)$ [4]

To conclude, we will investigate 3 GUTs, which along with the presence of a cosmological scalar field induce spacetime variations in the couplings. Also, we use the fact that in these models all varying quantities depend on the α variation, thus simplifying the parametric space of the models to $(R, S, \Delta\alpha/\alpha)$. Now we need to find a way to study GUTs in the context of compact objects, namely white dwarfs and neutron stars.

4

Compact Objects

Compact objects encompass a diverse array of stellar remnants, ranging from white dwarfs to neutron stars and black holes. They constitute the forefront of research, due to their widely unexplained characteristics that cause extreme internal and external phenomena. With the advancement of technology and new infrastructure, researchers have been able to observe compact objects using different signals (electromagnetic and gravitational), which can be valuable to understanding them.

1. Formation

Compact objects are formed through the gravitational collapse of progenitor stars during their final evolutionary stages.[5] Depending on the initial mass of the star, the outcome of its collapse may vary.
More specifically during the last stages of their life cycle, low to medium-mass stars (up to about 8 $M_{\odot}$) exhaust all their hydrogen fuel, and thus their cores contract and heat up, while their outer layers expand. These red giant stars now burn helium and heavier elements in their cores and have lower effective temperatures. The continuously expanding stars will start to expel their outer layers into space forming a gas nebula that surrounds them. Eventually, what remains is the dense core, which gradually cools down to become a white dwarf.
More massive stars (greater than about 8 $M_{\odot}$) follow a different, and more violent, evolutionary path. These stars burn through their fuel at faster speeds due to their higher mass, leading to significantly shorter

lifetimes. When this occurs, their cores collapse under their own gravity in such a rapid and intense manner that it triggers a supernova. During this event, the outer layers of the star are ejected into space, leaving behind a highly compressed core. Finally, a neutron star is created when the core collapse is halted due to a mechanism, that will be discussed below.[6]
In the case of extremely massive stars (greater than about 15 $M_{\odot}$), gravity fully dominates and the core collapses into a single point, the black hole. From now on, we will only refer to the first two compact objects, since they are the main focus of this thesis.

2. Composition and equilibrium

Being former cores of stars, white dwarfs and especially neutron stars are extremely dense. They are small in size (about the size of the Earth and an asteroid respectively), but have masses comparable to that of (or bigger than) the Sun. Due to their different origin, neutron stars and white dwarfs have vastly different compositions. The former is primarily composed of densely packed neutrons, along with small fractions of protons, electrons, and possibly other particles such as muons [7, 6]. The intense gravitational forces present in their core, cause atomic nuclei to break down, forming a sea of neutrons. White dwarfs, on the other hand, are made up of nuclei such as carbon and oxygen, since gravity isn't sufficient to break down these atomic structures [5].

It is crucial to point out the dynamics of such objects and the occurring mechanisms against collapse. Unlike normal stars, compact objects don't rely on nuclear fusion to generate power and balance gravity. The mechanism counterbalancing gravitational collapse is electron degeneracy pressure for white dwarfs and neutron degeneracy pressure for neutron stars. Since electrons and neutrons are fermions, they abide by Pauli's exclusion principle, which states that no two fermions with the same quantum numbers should exist in the same system. So, as gravity compresses matter towards the center, fermions are squeezed into confined spaces, and their energies become quantized. Eventually, the available energy levels (energies lower than the Fermi energy) become so closely spaced that the fermions begin to fill them up completely, reaching a state of degeneracy. Since fermions cannot jump to higher states, this phenomenon creates an outward pressure that equalizes the inward pull

of gravity and stabilizes the star.

In a common star, this interplay between gravity and outward pressure is explained mathematically by the 4 differential equations of equilibrium (hydrostatic equilibrium, mass conservation, temperature gradient, and luminosity gradient dependent on nuclear reactions). In compact objects, we utilize only 2 of them since energy-generating mechanisms don't exist at their cores. These are the following (assuming additional relativistic corrections):

$$\frac{dp}{dr} = -\frac{G\rho(r)M(r)}{r^2}\left[1+\frac{p(r)}{\epsilon(r)}\right]\left[1+\frac{4\pi r^3 p(r)}{M(r)c^2}\right]\left[1-\frac{2GM(r)}{c^2 r}\right]^{-1} \tag{4.1}$$

$$\frac{dM}{dr} = 4\pi r^2 \rho(r) \tag{4.2}$$

along with the initial conditions: $p(0) = p_c, M(0) = 0$

3. The Polytrope

Additionally, we require a pressure-energy density relation, which takes into account the state of matter in the interior. This equation of state differs amongst stars and can be modeled by approximations, as we will witness in the following chapters. The easiest EoS in terms of calculations, but also the only one for which there are analytical solutions to the system, is the polytropic equation of state. This EoS was derived by Chandrasekhar from the Lane-Emden equation [8]

$$\frac{1}{\xi^2}\frac{d}{d\xi}\left[\xi^2\frac{d\theta_n}{d\xi}\right] = -\theta_n^n \tag{4.3}$$

where $\rho(r) \equiv \rho_c[\theta_n(r)]^n$ and ξ, θ_n are the dimensionless length and density respectively, and n is the polytropic index [8]. There are only three analytical solutions for the Lane-Emden equation, namely the $n = 0, 1, 5$ cases. In the context of this analysis, we will use Chandrasekhar's numerical solutions [8] for the non-relativistic ($n = 3/2$) and relativistic ($n = 3$) limits. By solving eq. 4.3 we get the general polytropic equation $p = K\epsilon^\gamma = K\epsilon^{1+1/n}$, where $\epsilon = \rho c^2$ and K is a model-dependent constant. Considering the above, we get an equation of state for the non-relativistic case:

$$p = K_{NR}\epsilon^{5/3}, \tag{4.4}$$

where

$$K_{NR} = \frac{\bar{h}^2}{15\pi^2 m_e}\left(\frac{3\pi^2 Z}{m_N c^2 A}\right)^{5/3} \tag{4.5}$$

whereas for the relativistic case:

$$p = K_R \epsilon^{4/3}, \tag{4.6}$$

with

$$K_R = \frac{\bar{h}c}{12\pi^2}\left(\frac{3\pi^2 Z}{m_N c^2 A}\right)^{4/3} \tag{4.7}$$

Now that we have considered the properties of matter in the interior by deriving a $p = f(\epsilon)$ relation, we can tackle the TOV equations. Solving (eq.4.1,4.2) provides us with the Mass-Radius relation of a compact object:

$$M = 4\pi c^{(2n+2)/(n-1)}\left(\frac{(n+1)K}{4\pi G}\right)^{n/(n-1)} \xi_1^{(n-3)/(1-n)}\xi_1^2|\theta'(\xi_1)|R^{(3-n)/(1-n)} \tag{4.8}$$

where ξ_1 corresponds to the first zero of the dimensionless density θ [8].

4. Observations and measurements

Neutron stars and white dwarfs are excellent laboratories to test our present knowledge of the fundamental properties of matter under the influence of strong gravitational and magnetic fields at extreme densities, isospin asymmetry, and temperature. They offer an interesting interplay between nuclear processes and astrophysical observables. The new generation of space X-ray and γ-ray observatories are enabling new observations and breakthrough discoveries [6]. Thermal emissions from isolated neutron stars provide important information on their cooling history and allow for the determination of their radii. At the same time, improvements in radio telescopes and interferometric techniques have increased the number of known binary pulsars, allowing for extremely precise neutron star mass measurements and tests of general relativity.

After almost sixty years of observations, we have collected an enormous amount of data on different neutron star observables that include [6]: masses, radii, rotational periods, surface temperatures, gravitational redshifts, quasiperiodic oscillations, magnetic fields, glitches, timing noise, and very recently, gravitational waves. A large multinational effort has

taken place in the last decade to build a new generation of gravitational wave detectors which have been recently rewarded with the exciting observation of the first signal from the merger of two neutron stars.

The mass-to-radius measurement in neutron stars (and white dwarfs) is possibly the most important and versatile quantity that we can obtain from them at the moment. Amongst others, it can be utilized for studies of matter properties in extreme environments, astrophysical characteristics of compact objects, and tests of fundamental physics (e.g. the Standard Model and general relativity) [9]. In Fig.4.1, we present constraints on the mass-radius curve from observational data (both electromagnetic and gravitational). Mass measurements can be inferred directly from observations of binary systems and likely also from supernova explosions. Radii on the other hand are very difficult to measure mainly because compact objects are very small and far away from us. However, a possible way to determine them is to use the thermal emission of low-mass X-ray binaries, additionally considering mass measurements. The major uncertainties in radius calculation come from the determination of the temperature, which requires the assumption of an atmospheric model, and the estimation of the distance of the star.

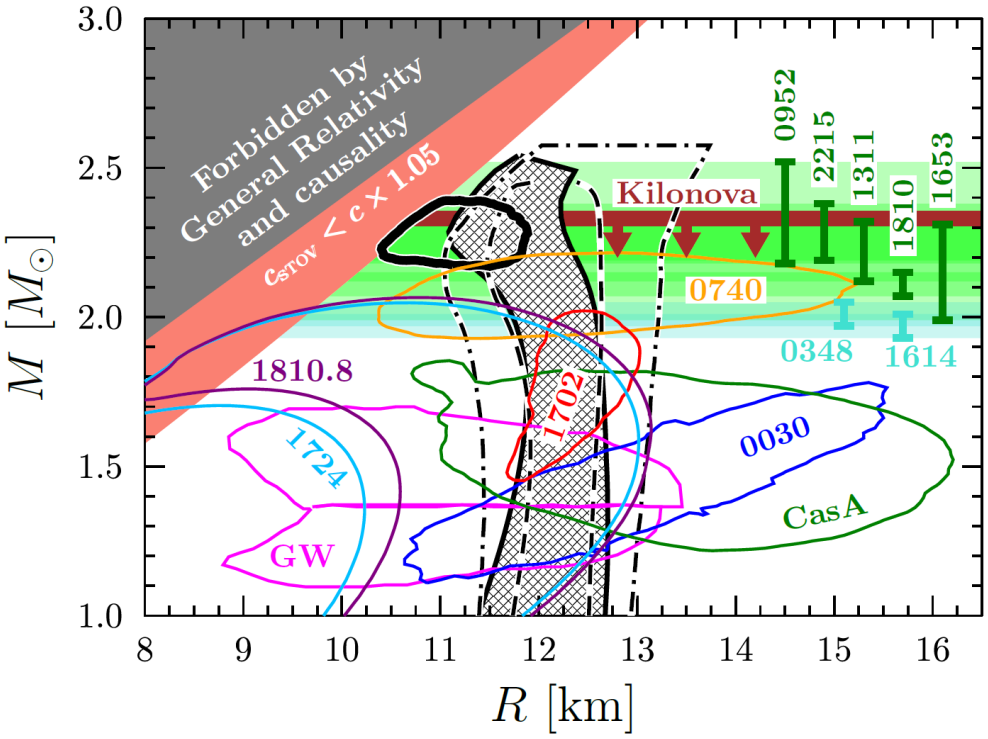

4.1: [10] Mass-Radius constraints from neutron star observations. Vertical bars and corresponding colored bars display 1σ mass ranges for neutron stars in binaries. The brown line shows the upper mass limit adopted from the GW 170817 measurement. The grey-shaded region is prohibited due to the "maximum compactness" criterion. The red-shaded region is also excluded, due to the speed of sound surpassing the speed of light in such neutron star cases. The cross-hatched region is formed by the 90% credible intervals for radii at given NS masses, obtained from fitting observational data. Thin dashed and dash-dotted 90% credible contours show similar results, by [11] and [12] respectively.

5

White Dwarfs

In this section, we will investigate the impact of varying couplings on white dwarfs. As explained in Chapter 4, white dwarfs are remnant cores of relatively low-mass stars ($< 8M_{\odot}$), stabilized by electron degeneracy pressure. They consist of carbon and oxygen and have a Chandrasekhar limit of approximately $1.4M_{\odot}$. The Chandrasekhar limit is the mass above which electron degeneracy pressure in the star's core is insufficient to balance the star's own gravitational self-attraction. We will use white dwarfs as a toy model, to gain some intuition on how varying α affects a degenerate star, and then move on to the more complicated neutron star model.

1. Perturbations

Compact objects are comprised of degenerate matter, which mainly consists of electrons and nucleons. As a result, variations in the strength of the electroweak interaction (or the fine structure constant) slightly shift the stars' equilibrium. We can model this as perturbations to the Mass-Radius relation. So initially, we express the electron and nucleon masses as dimensionless couplings, by comparing them to the Planck mass:

$$\alpha_i = \frac{Gm_i^2}{\hbar c}, \tag{5.1}$$

Now we have two choices: either particle masses can vary and the Planck mass (and therefore G) is fixed, or the opposite happens. In our anal-

ysis, we assume the first, but the opposite choice would be physically equivalent (i.e. it would yield the same results for observable quantities, although it would lead to a more complicated formalism). As a result, mass variations can be formulated as such:

$$\frac{\Delta\alpha_e}{\alpha_e} = 2\frac{\Delta m_e}{m_e} = (1+S)\frac{\Delta\alpha}{\alpha} \tag{5.2}$$

$$\frac{\Delta\alpha_N}{\alpha_N} = 2\frac{\Delta m_N}{m_N} = 2[0.8R + 0.2(1+S)]\frac{\Delta\alpha}{\alpha} \tag{5.3}$$

These perturbations need to be included in the TOV equations (eq.4.1, 4.2) as well as the Mass-Radius relation (eq.4.8), which can be accomplished using the following methodology. We will start with the easiest case of a polytrope and consider 2 scenarios: the non-relativistic and relativistic. In the next chapters, we expand upon this methodology for other EoS.

At first, we shift to Planck units, since they remain unchanged, and substitute masses with couplings using eq.5.1 (we note that in the Mass-Radius relation, only K has a particle mass dependency). In the non-relativistic case, eq.4.8 becomes:

$$M_*^{1/3} R_* = Q_{NR}\alpha_e^{-1/2}\alpha_N^{-5/6}, \tag{5.4}$$

where Q_{NR} is a dimensionless constant. Then, we Taylor expand for both couplings to add perturbations.

$$\left(\frac{M_*(\alpha)}{M_{*,0}}\right)^{1/3}\frac{R_*(\alpha)}{R_{*,0}} = 1 - x, \tag{5.5}$$

where the zero subscript indicates the standard quantity, while x is the perturbation dependent on the $(R, S, \Delta\alpha/\alpha)$ model

$$x = \left[\frac{4}{3}R + \frac{5}{6}(1+S)\right]\frac{\Delta\alpha}{\alpha} \tag{5.6}$$

Similarly in the relativistic case, we find

$$M_* = Q_R\alpha_N^{-1} \tag{5.7}$$

and therefore

$$\frac{M_*(\alpha)}{M_{*,0}} = 1 - y \tag{5.8}$$

where again

$$y = \left[\frac{8}{5}R + \frac{2}{5}(1+S)\right]\frac{\Delta\alpha}{\alpha} \tag{5.9}$$

Applying the same methodology to the non-relativistic TOV equations:

$$\frac{dp_*}{dr*} = -O_1 \frac{m_* p_*^{3/5}}{r_*^2} \alpha_e^{3/10} \alpha_N^{1/2} \left[1 + \frac{3}{5}x\right] \tag{5.10}$$

$$\frac{dm_*}{dr_*} = O_2 r_*^2 p_*^{3/5} \alpha_e^{3/10} \alpha_N^{1/2} \left[1 + \frac{3}{5}x\right] \tag{5.11}$$

and for the relativistic case (without corrections):

$$\frac{dp_*}{dr*} = -O_3 \frac{m_* p_*^{3/4}}{r_*^2} \alpha_N^{1/2} \left[1 + \frac{1}{2}y\right] \tag{5.12}$$

$$\frac{dm_*}{dr_*} = O_4 r_*^2 p_*^{3/4} \alpha_N^{1/2} \left[1 + \frac{1}{2}y\right] \tag{5.13}$$

where x, y are defined in eq.5.6 and 5.9 respectively. It is also important to note that the above perturbations don't affect the zero-order term (the general form of the equations), so we can always revert the equations back to the original units and add the corrections. Now, observing the relativistic corrections in the equation of hydrostatic equilibrium (eq.4.1, 4.2), it becomes clear that only the first term has an α dependency. As a result, it is perturbed as follows for the non-relativistic case:

$$1 + \frac{p}{\epsilon} \to 1 + \frac{O p_*^{2/5}}{\alpha_e^{3/10} \alpha_N^{1/2}} \left[1 - \frac{3}{5}x\right] \tag{5.14}$$

while for the relativistic case, we get:

$$1 + \frac{p}{\epsilon} \to 1 + \frac{O p_*^{1/4}}{\alpha_N^{1/2}} \left[1 - \frac{1}{2}y\right] \tag{5.15}$$

Now that we have produced the equations describing the behavior of polytropes under a varying α regime, we can begin testing this model for various cases.

2. Results

We initially assume an α variation of the order of 10^{-3} which is small enough to act as a perturbation. We will investigate bigger values of $d\alpha/\alpha$ later. We also allow for both positive and negative variations, to determine if the perturbed models are symmetrical to the unperturbed

white dwarf. In Figure 5.1, we observe the results for the non-relativistic as well as the relativistic case for the Unification model $(R = 36, S = 160)$. Both plots agree on the fact that a negative $d\alpha/\alpha$ increases the mass and radius of the star, while a positive variation causes the opposite effect. This phenomenon can be justified since the strength of the electroweak interaction, and thus the electron degeneracy pressure is related to α. On the other hand, (R, S) values affect the QCD scale (proton and neutron masses) and the electroweak interaction respectively. So, a positive variation of α alone would mean stronger degeneracy pressure and thus lead to a more massive star. In the unification model, this effect is overshadowed by the simultaneous increase in the QCD scale, due to a positive R. As a result, we observe a decrease in the mass of the white dwarf, since the mass of individual nucleons is now increased with respect to electron degeneracy pressure and the star must shed matter to reach equilibrium. For the relativistic case, it is important to note that the Chandrasekhar limit is also shifted to lower or higher masses respectively. It is also clear that perturbed cases in the relativistic model aren't symmetric to the unperturbed case. This occurs due to the perturbation added to one of the correction terms in the hydrostatic equilibrium equation (eq.4.1).

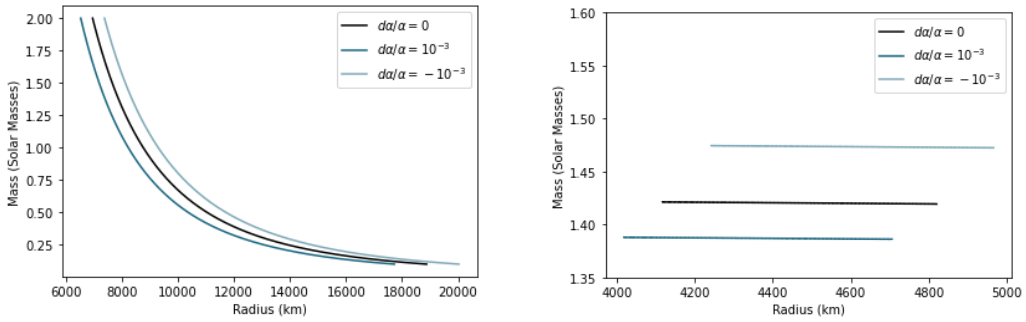

5.1: Mass-Radius relation for the Unification scenario $(R = 36, S = 160)$ in the non-relativistic (left) and relativistic (right) case for positive and negative variations of α. The relativistic plot also indicates the Chandrasekhar limit.

A similar behavior can be seen in Figure 5.2, describing results for the Dilaton case $(R = 109.4, S = 0)$. This time the bigger positive R value dominates significantly over the alpha variation, causing more exaggerated shifts from the unperturbed case. In this model, for a negative α variation we observe a Chandrasekhar limit at about $1.5M_{\odot}$, significantly bigger than the mass of ZTF J1901+1458, the most massive white dwarf ever detected $(1.327–1.365M_{\odot})$ [13]. Thus, so far observations indicate

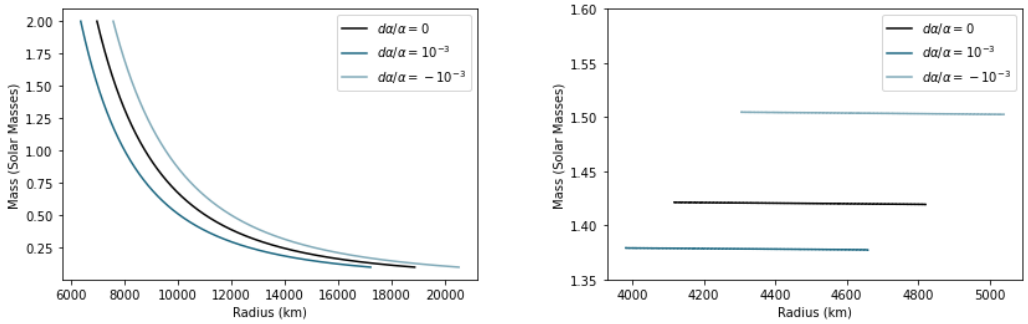

5.2: Mass-Radius relation for the Dilaton scenario $(R = 109.4, S = 0)$ in the non-relativistic (left) and relativistic (right) case for positive and negative variations of α.

that a Dilaton model with a negative α variation at the 10^{-3} level is unrealistic.

The UV-Cutoff scenario $(R = -183, S = 22.5)$ presents us with entirely different results. In Figure 5.3, we can see that the behaviors corresponding to symmetric α variations are now reversed, with the positive α variation resulting in an increase in mass and radius. The negative R value in this model reduces the QCD scale, while for a positive $d\alpha/\alpha$, electron degeneracy pressure is increased. The above phenomena have a cumulative effect on the mass of a star, amplifying the gap from the standard case in the relativistic white dwarf. On the other hand, the negative $d\alpha/\alpha$ scenario is the outcome of clashing events, specifically a decrease both in the degeneracy pressure and the QCD scale.

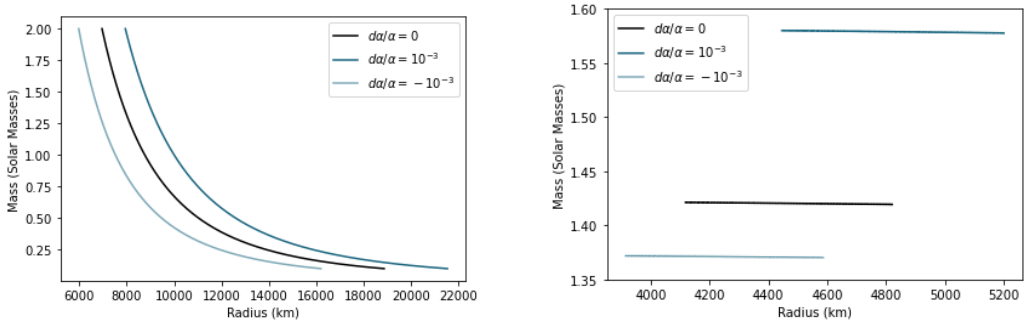

5.3: Mass-Radius relation for the UV-Cutoff scenario $(R = -183, S = 22.5)$ in the non-relativistic (left) and relativistic (right) case for positive and negative variations of α.

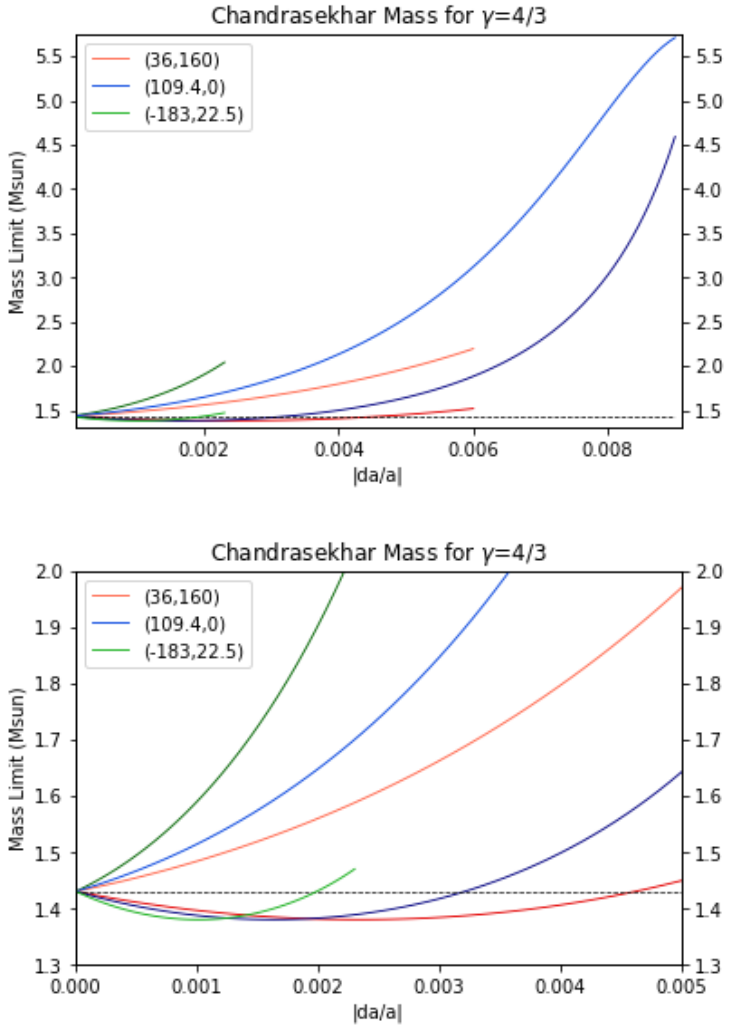

5.4: The Chandrasekhar mass limit as a function of the absolute α variation for the 3 GUT models. Lighter shades indicate a negative α variation, while darker shades correspond to positive $d\alpha/\alpha$. Due to code limitations and the perturbations becoming comparable to the zero-order term, each GUT model is characterized by a different $|d\alpha/\alpha|$ domain, where solving the problem is possible. The second Figure is a zoom-in of the bottom left corner of the first Figure, and the dotted line shows the unperturbed Chandrasekhar limit.

This argument justifies the relatively small deviation from the unperturbed case, that can be observed for negative $d\alpha/\alpha$.

A more detailed investigation into the Chandrasekhar mass is shown in Figure 5.4 where we perform the same analysis as before, with the exception that now $d\alpha/\alpha$ is a free parameter. As a consistency check, when $d\alpha/\alpha$ equals 10^{-3} we recover the same results for the mass limit as the ones in Figures 5.1, 5.2, 5.3. For increasing absolute α variations, the first-order term in equations 5.12, 5.13, 5.15 starts becoming comparable to or even bigger than the zero-order term. If this didn't occur, we would expect monotonous behaviors for models that are initially below the standard Chandrasekhar limit as well as more moderate slopes after some $|d\alpha/\alpha|$ value.

6

Neutron Stars I: Methodology

1. Perturbations

As derived in the previous Chapter, the Mass-Radius relation in the non-relativistic limit is the following:

$$M_*^{1/3} R_* \propto \frac{1}{\alpha_e^{1/2} \alpha_N^{5/6}}, \tag{6.1}$$

while for the relativistic limit, we have:

$$M_* \propto \frac{1}{\alpha_N}. \tag{6.2}$$

Since we are assuming that perturbations are small, we can interpolate between the two cases to acquire this more general relation:

$$M_*^{n-1} R_*^{3-n} \propto \frac{1}{\alpha_e^{(3-n)/2} \alpha_N^{(1+n)/2}} \tag{6.3}$$

the proportionality factor will depend on the equation of state, which we will discuss below. So the perturbed case should be

$$\left(\frac{M_*(\alpha)}{M_{*,0}}\right)^{(n-1)} \left(\frac{R_*(\alpha)}{R_{*,0}}\right)^{(3-n)} = 1 - z \tag{6.4}$$

where

$$z = \left[\frac{4}{5}(n+1)R + \frac{17-3n}{10}(1-S)\right] \frac{\Delta\alpha}{\alpha}, \tag{6.5}$$

from which we can recover the two previous limits. This approach is purely phenomenological, meaning that the polytropic index or the Mass-Radius relation as a whole doesn't necessarily have physical meaning.

From the TOV equations, we also need to parameterize the behavior of K, and by demanding that it has the correct physical dimensions, namely $m^{1/n}s^{2/n}/(kg)^{1/n}$, in addition to the two limits, we can find:

$$K \propto \frac{\bar{h}^{3/n}}{m_e^{-1+3/n} m_N^{1+1/n} c^{5/n}}. \tag{6.6}$$

A similar interpolation can be done for the TOV equations, which become

$$\frac{dp_*}{dr_*} = -O\frac{m_* p_*^{\frac{n}{1+n}}}{r_*^2} \alpha_e^{\frac{3-n}{2(1+n)}} \alpha_N^{1/2}(1+A) \tag{6.7}$$

$$\frac{dm_*}{dr_*} = O r_*^2 p_*^{\frac{n}{1+n}} \alpha_e^{\frac{3-n}{2(1+n)}} \alpha_N^{1/2}(1+A), \tag{6.8}$$

where

$$A = \left[\frac{4}{5}R + \frac{17-3n}{10(1+n)}(1+S)\right]\frac{\Delta\alpha}{\alpha} \tag{6.9}$$

where we notice that $z = (1+n)A$. Finally, for the first of the relativistic corrections in the TOV equation, we have

$$1 + \frac{p}{\epsilon} \to 1 + \frac{O p_*^{\frac{n}{1+n}}}{\alpha_e^{\frac{3-n}{2(1+n)}} \alpha_N^{1/2}}(1-A). \tag{6.10}$$

It is important to note that now the perturbation terms (eq.6.5, 6.9) are not only dependent on the GUT model and α variation - there is an additional dependency on the polytropic index.

2. Numerical EoS

Apart from standard analytical equations which describe the interior of a compact object, there are more accurate EoS in the form of numerical tables. These offer more versatility since they don't assume the same behavior of matter in different depths from the surface of the star. Given that the pressure gradient in a neutron star is significant, we should account for phase transitions as well as relativistic or hyper-relativistic

	Quantity	Value
n_S	saturation density in symmetric matter	$0.159\ fm^{-3}$
E_0	binding energy per baryon in saturation	$515.97\ MeV$
K	incompressibility	$230\ MeV$
K'	skewness	$-363.11\ MeV$
J	symmetry energy	$32.04\ MeV$
L	symmetry energy slope parameter	$46.00\ MeV$
K_{sym}	symmetry incompressibility	$-119.73\ MeV$

6.1: Nuclear matter properties for the SLY4 EoS [15, 16, 17]

	Quantity	Value
M_{max}	maximum mass	$2.075\ M_{sun}$
R_{Mmax}	radius at maximum NS mass	$10.09\ km$
$R_{1.4}$	radius at $1.4M_{sun}$ NS mass	$11.86\ km$

6.2: Neutron star properties for the SLY4 EoS [15, 16, 17]

phenomena near the center of the star. This can be accomplished using numerical EoS. Here we utilize the SLY4 model, acquired from the CompOSE database [14]. SLY4 is a stiff EoS that assumes degenerate matter comprised of nucleons and electrons. Nuclear as well as neutron star properties for this model are shown in Tables 6.1, 6.2. Figure 6.1 represents the general behavior of the SLY4 EoS.

The main issue with numerical EoS in our analysis is that, so far, we have only perturbed the model using analytical EoS expressions. More specifically, eq. 6.7, 6.8 directly imply the use of a polytrope, or at least some EoS parametrized as a polytrope. Consequently, we need to approximate the numerical EoS in a way that will enable us to use it in the perturbed TOV equations. We follow the methodology described below:

- First, we discretize the (p, ϵ) parametric space into equal steps.
- We fit a polytrope into every one of these steps and run tests with discretization to recover the option that best fits the CompOSE data for SLY4. Such tests are presented in Figure 6.2 where, as expected, a smaller step produces a better fit.
- Now our numerical EoS (pressure and energy density data) is transformed into a (n_i, K_i) table, where n_i, K_i are the polytropic index and polytropic coefficient for step i respectively. As a result, we have approximated our EoS using polytopic parameters, which can

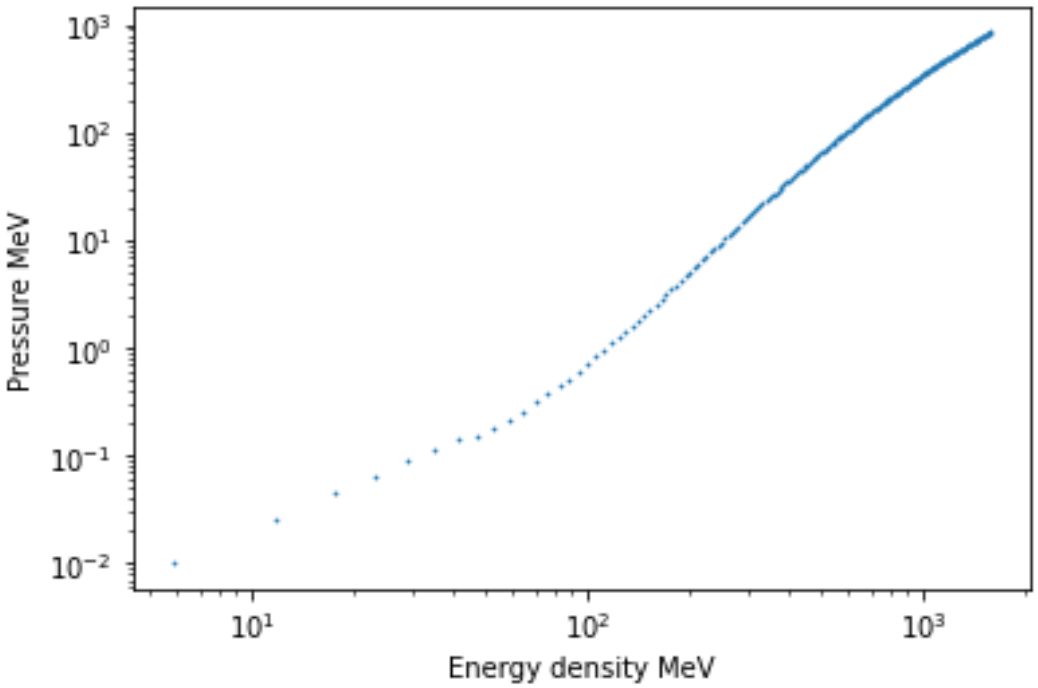

6.1: The SLY4 EoS, produced using the CompOSE software. The first datapoint $(p, \epsilon) = (2.14325 \times 10^{-8} MeV, 9.30754 \times 10^{-5} MeV)$ is not pictured, to allow for a better representation of the general behavior of this EoS.

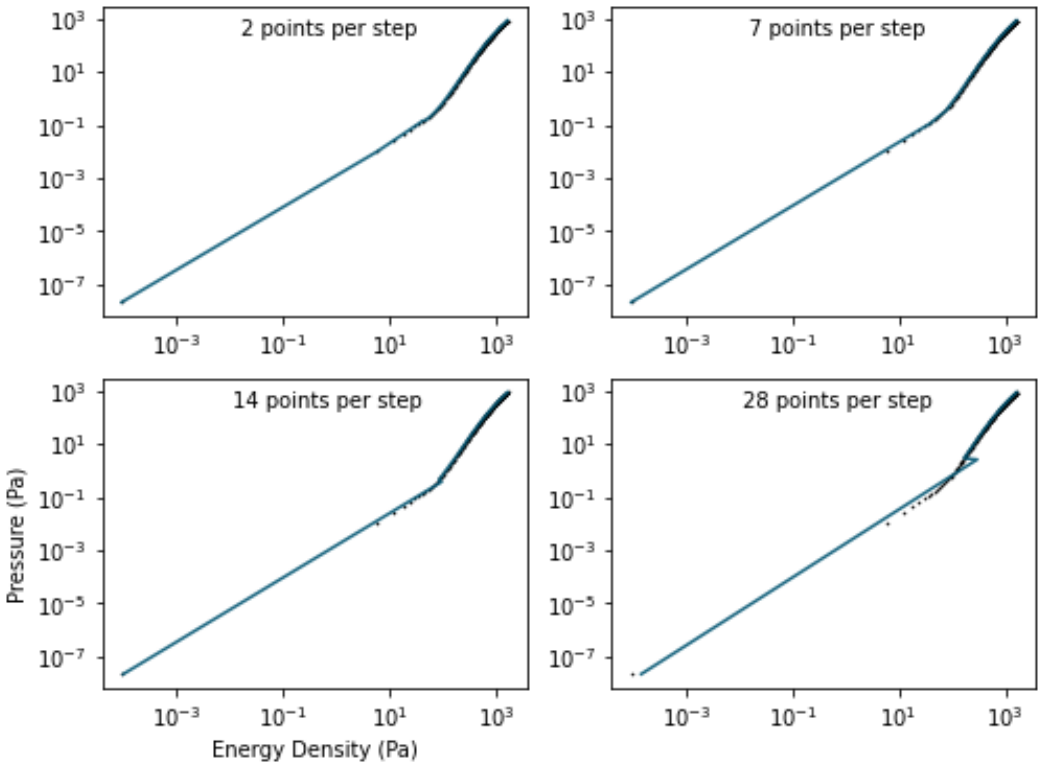

6.2: Discretization tests for approximating the behavior of the SLY4 EoS. It is obvious from the plots above that a smaller stepsize improves the approximation and thus produces a more accurate result.

be used to solve the TOV equations. It is important to note that the (n_i, K_i) are merely phenomenological parameters, that is they don't hold any physical meaning about the properties of matter. As a result, n values outside the relativistic and non-relativistic limits are allowed.

- Previously, we utilized built-in Python solvers for the TOV problem. But now, since the polytrope changes for each step, as we move from the center of the star outwards, we require an algorithm that allows for the manipulation of parameter values with every step. As a result, we create an algorithm from scratch based on the 4th-order Runge-Kutta method (see Appendix B).

Through the steps described above, we have managed to extend our analysis on neutron stars with numerical EoS. In the next Chapter, we investigate GUT models in this context.

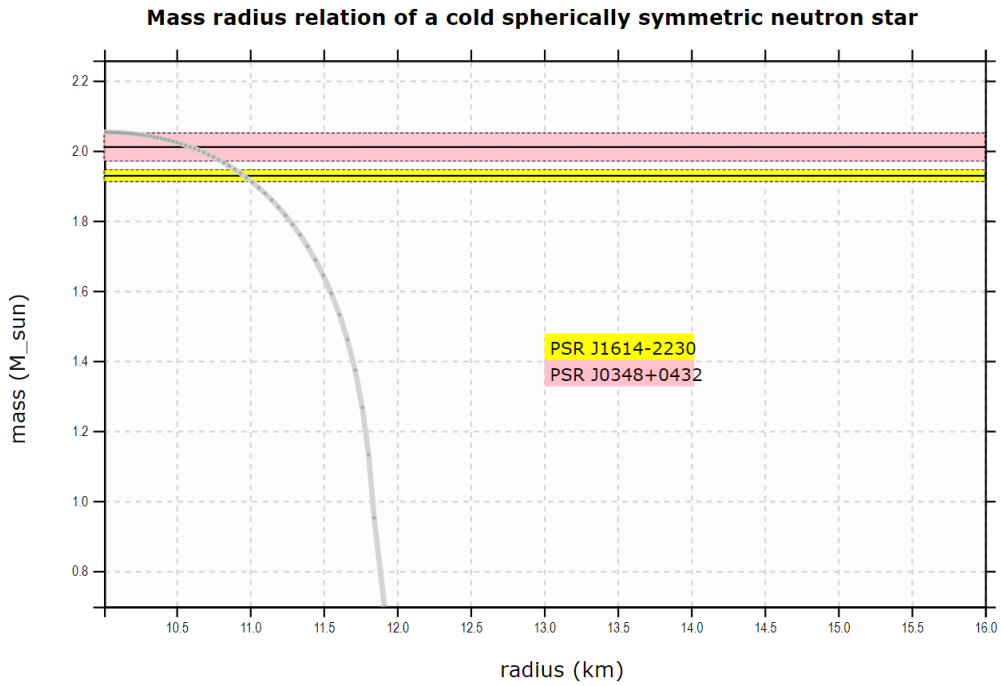

6.3: Mass-Radius relation of a cold symmetric neutron star with a SLY4 EoS, acquired from the CompOSE database website [14]. Horizontal lines with pink and yellow error bars represent pulsar measurements.

7

Neutron Stars II: Results

We follow the same procedure as in the white dwarf model in Chapter 5, investigating 3 different GUT cases. We use the previous methodology to produce results for the SLY4 EoS, assuming only positive and negative perturbations of the order of 10^{-3}. As a consistency check, we can compare the unperturbed black lines from Figures 7.1, 7.2, 7.3 to Figure 6.3, which depicts the Mass-Radius relation for the SLY4 EoS. We observe an almost perfect alignment. Attempts of plotting similar figures using the TOVsolver code [18], again without perturbations, yielded Mass-Radius relations that differed significantly from the original Figure 6.3.

In Figure 7.1 we observe results for the Unification case $(R, S) = (36, 160)$. It is demonstrated again that negative perturbations raise the mass and radius of the star, whereas positive variations have the opposite effect. It is reasonable to recover similar results to the polytropic white dwarf since neutron stars rely on the gravity-degeneracy pressure equilibrium for stability. Consequently, the GUT model and α variation will affect the QCD scale and neutron degeneracy pressure respectively, leading to a shift in the equilibrium and the Mass-Radius relation. Figures 7.2, 7.3 depict the Dilaton $(R, S) = (109.4, 0)$ and UV-Cutoff $(R, S) = (-183, 22.5)$ models, where we observe more exaggerated shifts from the unperturbed case for the same reasons described in Chapter 5. Also in Figure 7.3, the behaviors of positive and negative α variations are reversed due to the negative R and relatively small S parameters in the GUT model. Another expected result is the asymmetry of the perturbed cases, which is more visible in the last Figure but evident in all 3 due to the additional perturbation in the first relativistic correction.

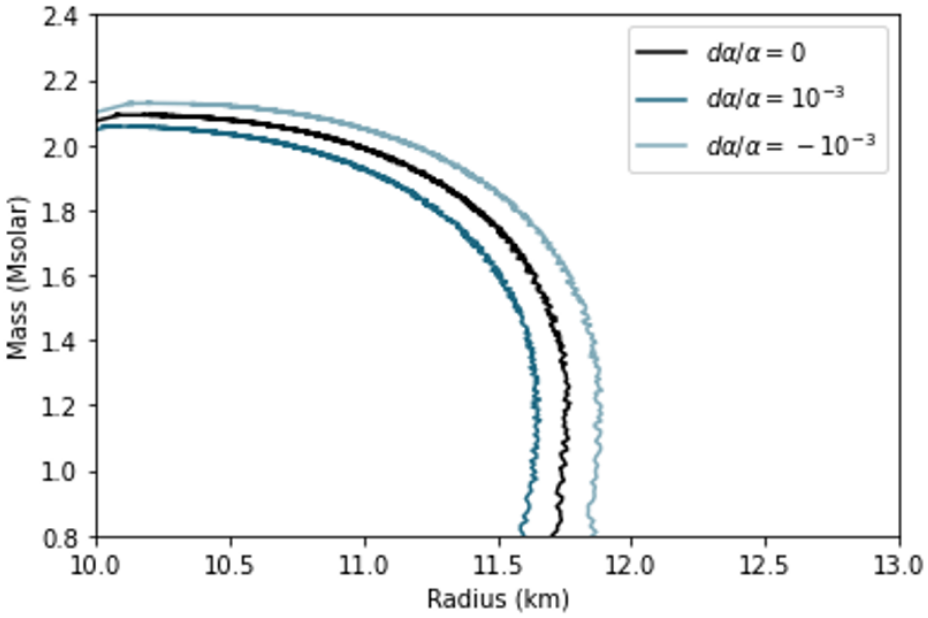

7.1: Mass-Radius relation for the Unification model $(R, S) = (36, 160)$. Positive and negative variations of α are depicted in dark and light blue respectively.

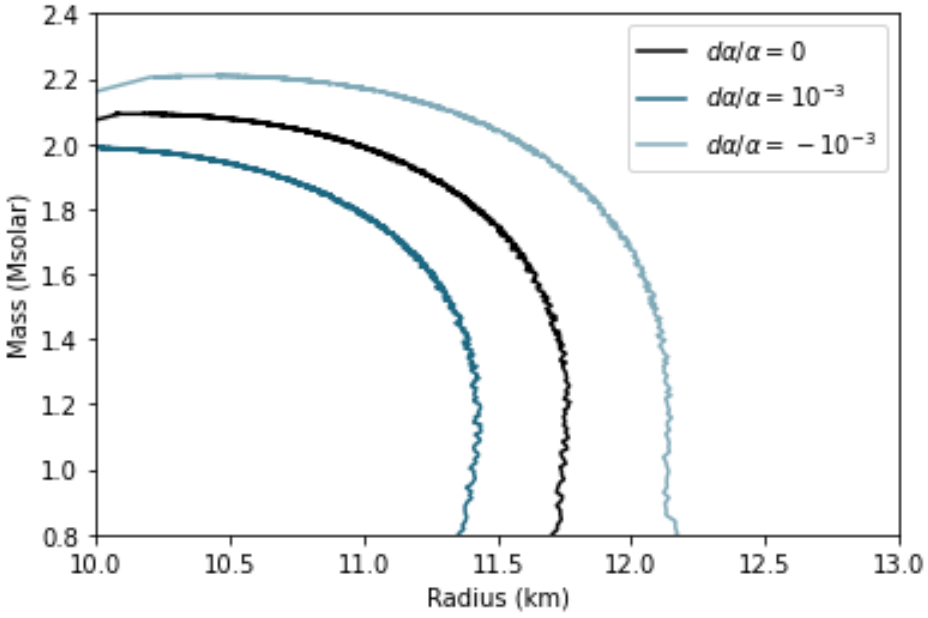

7.2: Mass-Radius relation for the Dilaton model $(R, S) = (109.4, 0)$. Positive and negative variations of α are depicted in dark and light blue respectively.

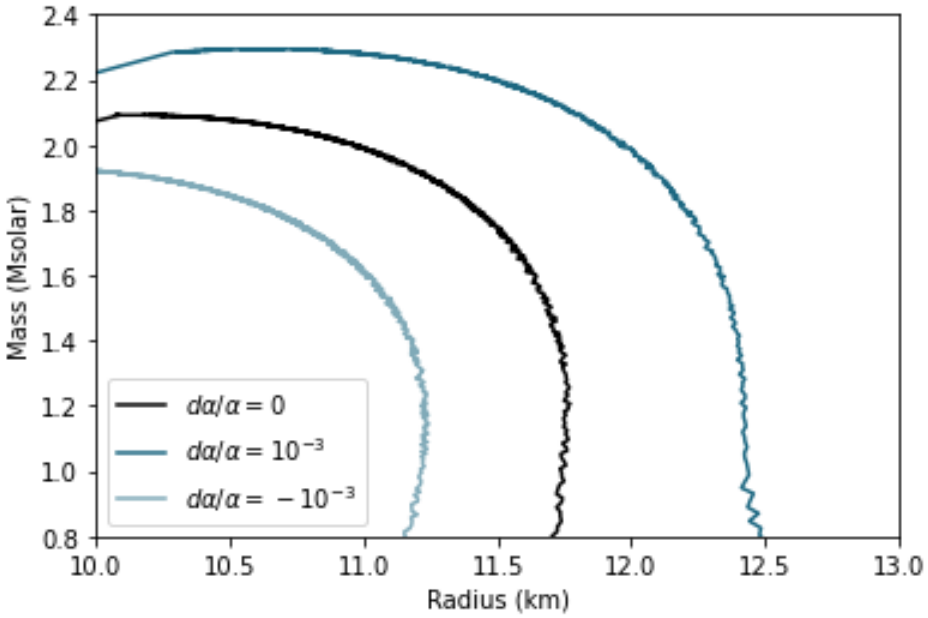

7.3: Mass-Radius relation for the UV-Cutoff model $(R, S) = (-183, 22.5)$. Positive and negative variations of α are depicted in dark and light blue respectively.

8

Conclusions

This thesis has been an attempt to clarify the efforts of theorists and experimentalists in search of a great theory that adequately describes the world, from the smallest scales to the largest. We focused on a particular group of models, Grand Unified Theories, which amongst other physical consequences, predict the unification of electroweak and strong interactions in a specific energy point, dependent on the (R, S) pair. We selected 3 distinct examples in an attempt to cover a wide range of the parametric space, in addition to including a variation of the fine structure constant α. To test these theories, we utilized degenerate objects as probes, namely white dwarfs and neutron stars. Being stellar remnants, these stars don't depend on nuclear fusion to combat gravitational collapse but instead rely on degeneracy pressure. They can be modeled using the Tolman-Oppenheimer-Volkov (TOV) equations in addition to an equation of state (EoS). Because GUT models affect the dynamics of a degenerate star, we modeled their effects as perturbations to the TOV equations.

Beginning our analysis with white dwarfs, we followed a methodology that includes Taylor expanding the TOV equations and using a polytope as the EoS. We compared our results for the 3 example GUT models and also for symmetric variations of α. We found that positive perturbations tend to reduce the mass of a star, both in the relativistic and non-relativistic limits. In addition, we observed an asymmetry between positive and negative variations in the relativistic star, which occurs due to the additional perturbation in a relativistic correction on the TOV equations. By comparing our results with a measurement of the most

massive white dwarf detected so far, we determined that a Dilaton model with a negative variation at the 10^{-3} level is an unlikely scenario. A more detailed analysis of the Chandrasekhar mass indicated that there is an upper limit on the absolute value of the fine structure constant variation. Future comparison with atomic clock data could provide further insight into this limit.

For the neutron star case, we interpolated and extrapolated between the previously derived Mass-Radius relations to recover a more general formula, where the perturbation depended on the EoS. Since we utilized a numerical EoS for this model, we had to parameterize it using the polytropic index and coefficient, to allow it to be used along the perturbed equations. The polytropic parameters of the EoS change as we move from the center of the star outwards, so for that reason, we created a solver that accounts for such changes. The results acquired from this analysis were almost identical to the white dwarf model, indicating that our methodology is consistent.

Nevertheless, many aspects of this work require improvement and further expansion. Firstly, the solver for the neutron star model with the numerical EoS needs to be rewritten in a more compact and simplified form, to reduce running times and enhance readability by other users. Also, thus far we have only investigated 3 very different GUT models, which hardly provide us with an intuition about the rest of the (R, S) parametric space. So, to perform a more comprehensive analysis we have to scan a bigger part of the parametric space. In addition, we can compare our results with reality, by utilizing α variation measurements or Mass-Radius measurements from neutron stars. This has already been achieved in [9] but taking into account recent advances in neutron star detection and measurements, we can build upon this work by utilizing this new data. Combining the theoretical model with measurements will enable us to constrain the entire GUT parametric space with the use of statistical methods.

Bibliography

[1] C J A P Martins. "The status of varying constants: a review of the physics, searches and implications". In: *Rep. Prog. Phys.* 80 (2017). DOI: 10.1088/1361-6633/aa860e.

[2] Alain Coc et al. "Coupled variations of fundamental couplings and primordial nucleosynthesis". In: *Physical Review D—Particles, Fields, Gravitation, and Cosmology* 76 (2007). DOI: 10.1103/PhysRevD.76.023511.

[3] Bruce A Campbell and Keith A Olive. "Nucleosynthesis and the time dependence of fundamental couplings". In: *Physics Letters B* 345 (1995). DOI: 10.1016/0370-2693(94)01652-S.

[4] Taekoon Lee. "A model for time-evolution of coupling constants". In: *Phys. Lett. B* 849 (2024). DOI: 10.1016/j.physletb.2023.138424.

[5] Irina Sagert et al. "Compact Objects for Undergraduates". In: *Eur. J. Phys.* 27 (2006). DOI: 10.1088/0143-0807/27/3/012.

[6] Isaac Vidaña. "A short walk through the physics of neutron stars". In: *European Physical Journal Plus.* 133 (2018). DOI: 10.1140/epjp/i2018-12329-x.

[7] J.M. Lattimer and M. Prakash. "The Physics of Neutron Stars". In: *Science* 304 (2004). DOI: 10.1126/science.1090720.

[8] S. Chandrasekhar. *An Introduction to the Study of Stellar Structure.* University of Chicago Press, 1938.

[9] D.M.N. Magano, J.M.A. Vilas Boas, and C.J.A.P. Martins. "Current and Future White Dwarf Mass-radius Constraints on Varying Fundamental Couplings and Unification Scenarios". In: *Phys. Rev. D* 96 (2017). DOI: 10.1103/PhysRevD.96.083012.

[10] Dmitry D. Ofengeim, Peter S. Shternin, and Tsvi Piran. "A three-parameter characterization of neutron stars' mass-radius relation and equation of state". In: (Apr. 2024). arXiv: 2404.17647 [astro-ph.HE].

[11] E. Annala and J. Hirvonen et al. T. Gorda. “Strongly interacting matter exhibits deconfined behavior in massive neutron stars”. In: *Commun* 14 (2023). DOI: 10.1038/s41467-023-44051-y.

[12] Len Brandes, Wolfram Weise, and Norbert Kaiser. “Evidence against a strong first-order phase transition in neutron star cores: Impact of new data”. In: *Phys. Rev. D* 108 (2023). DOI: 10.1103/PhysRevD.108.094014.

[13] Ilaria Caiazzo et al. “A highly magnetized and rapidly rotating white dwarf as small as the Moon”. In: *Nature* 596 (2021). DOI: 10.1038/s41586-021-03615-y.

[14] *CompOSE, RG(SLY4)*. URL: https://compose.obspm.fr/eos/134.

[15] Paweł Danielewicz and Jenny Lee. “Symmetry energy I: Semi-infinite matter”. In: *Nuclear Physics A* 818 (2009). DOI: 10.1016/j.nuclphysa.2008.11.007.

[16] F. Gulminelli and Ad. R. Raduta. “Unified treatment of subsaturation stellar matter at zero and finite temperature”. In: *Phys. Rev. C* 92 (2015). DOI: 10.1103/PhysRevC.92.055803.

[17] E. Chabanat et al. “A Skyrme parametrization from subnuclear to neutron star densities Part II. Nuclei far from stabilities”. In: *Nuclear Physics A* 635 (1998). DOI: 10.1016/S0375-9474(98)00180-8.

[18] *TOVsolver*. URL: https://github.com/amotornenko/TOVsolver.

A

White Dwarf Code

```
import numpy as np
import matplotlib.pyplot as plt
from scipy.integrate import solve_ivp

MeV2kg=1.78266269594644e-30
Msun=1.9891e30 #kg
kg2Msun=1/Msun
m2km=1e3
km2m=1e-3
Pa2dyne_cm2=10

pi=np.pi
G=6.6743e-11 # kg^(-1)*m^3*s^(-2)
c=3.0e8 #m*s^(-1)
Ro=G*Msun/c**2 # m
h=6.62607015e-34 # kg*m^2*s^(-1)
h_=h/(2*pi)
me=0.51099895000*MeV2kg # kg
A_Z=2
e0=me**4*c**5/(pi**2*h_**3) # kg*m^(-1)*s^(-2) => Pa
mp=938.27208816*MeV2kg # kg
mn=939.5654205*MeV2kg # kg
mN=(mp+mn)/2 # kg
N=1000

#ALL CONSTANTS ARE IN SI (Kg,J,s,m,Pa)

####################
#NEWTONS EQUATIONS (as is)
def linear_system_Newton(r,p_m):
    p,m=p_m #everything in SI
    g=5./3.
    K=h_**2./(15.*pi**2.*me)*(3.*pi**2./(mN*c**2.*A_Z))**(5./3.)
```

```
    e=(p/K)**(1/g)
    dp_dr=-G*e*m/(c**2*r**2)
    dm_dr=4*pi*r**2*e/c**2
    # print([dp_dr,dm_dr,r,K])
    return [dp_dr,dm_dr]

r=np.linspace(1e-6,11.45e6,N)
sol = solve_ivp(linear_system_Newton,(1e-10,11.45e6),[2.33002e21,0],method='RK45',t_eval=r,rtol=1e-6,atol=1e-10)
pr,ma=sol.y

fig, ax1 = plt.subplots()

color = 'tab:blue'
ax1.set_xlabel('r (m)')
ax1.set_ylabel('Pressure (dyne/cm^2)', color=color)
ax1.plot(r, pr*Pa2dyne_cm2, color=color, label='Pressure')
ax1.tick_params(axis='y', labelcolor=color)

# Creating a twin Axes for the mass on the right y-axis
ax2 = ax1.twinx()
color = 'tab:red'
ax2.set_ylabel('Mass (Mo)', color=color)
ax2.plot(r, ma/Msun, color=color, label='Mass')
ax2.tick_params(axis='y', labelcolor=color)
plt.show()


####################
# TOV EQUATIONS (as is)
def linear_system_TOV(r,p_m,g):
    p,m=p_m #everything in SI
    if g==5/3:
        K=h_**2./(15.*pi**2.*me)*(3.*pi**2./(mN*c**2.*A_Z))**(5./3.)
    elif g==4/3:
        K=h_*c/(12.*pi**2.)*(3.*pi**2./(mN*c**2.*A_Z))**(4./3.)
    else:
        raise ValueError("Unsupported value of g")
    e=(p/K)**(1/g)
    p_e=K*e**(g-1)
    dp_dr=-G*e*m/(c**2*r**2) * (1+p_e) * (1+4*pi*r**3*p/(m*c**2)) * \
            (1-2*G*m/(c**2*r))**(-1)
    dm_dr=4*pi*r**2*e/c**2
    # print([dp_dr,dm_dr,r]
    return [dp_dr,dm_dr]
R=110
S=0
da_a=0.001
g=5/3
```

```
if g==4/3: #relativistic
    initial_p=5.62e24
    rstart=1e-2
    rend=5.2e6
    gtxt='4/3'
elif g==5/3: #nonrelativistic
    initial_p=2.33002e21
    rstart=1e-6
    rend=11e6
    gtxt='5/3'
else:
    raise ValueError("Unsupported value of g")
r=np.linspace(rstart,rend,N)
sol=solve_ivp(linear_system_TOV,(rstart,rend),[initial_p,1e-10],
   method='RK45',t_eval=r,rtol=1e-6,atol=1e-10,args=(g,))
pr,ma=sol.y

fig, ax1 = plt.subplots()

color = 'tab:blue'
ax1.set_xlabel('r (km)')
ax1.set_ylabel('Pressure (dyne/cm^2)', color=color)
ax1.plot(r*1e-3, pr*Pa2dyne_cm2, color=color, label='Pressure')
ax1.tick_params(axis='y', labelcolor=color)

# Creating a twin Axes for the mass on the right y-axis
ax2=ax1.twinx()
color='tab:red'
ax2.set_ylabel('Mass (Mo)',color=color)
ax2.plot(r*1e-3,ma/Msun,color=color,label='Mass')
ax2.tick_params(axis='y',labelcolor=color)
plt.show()


####################
# NEWTON'S EQUATIONS (as is + with varying couplings)
N=1000
def K(n):
    if n==3:
        return h_*c/(12.*pi**2.)*(3.*pi**2./(mN*c**2.*A_Z))
    **(4./3.)
    elif n==3/2:
        return h_**2./(15.*pi**2.*me)*(3.*pi**2./(mN*c**2.*A_Z))
    **(5./3.)
p0_r=np.linspace(1e23,1e26,N) #central pressures
p0_n=np.linspace(1e20,4.5e21,N)
M=np.linspace(0.1*Msun,2*Msun,N) #for Mass - Radius relation
dencrit=mn*me**3*A_Z*c**3/(3*pi**2*h_**3)
ksi1_r=6.89685
ksi1_n=3.65375
ksi1_theta_r=2.01824
```

```
ksi1_theta_n=2.71406
Rad_r=np.zeros([N,2])
Rad_n=np.zeros([N,2])
M_r=np.zeros([N,2])
M_n=np.zeros([N,2])
RM=np.zeros([N,2]) # non relativistic only - there is no such
    relativistic relation
da_a=0.001
R=110
S=0
# def A(n):
#     return (n+1)**n/(4*pi)*ksi1_r**(3-n)*ksi1_theta_r**(1/(n-1))
x=(0.8*R+0.2*(1+S))*da_a
y=2*(0.8*R+0.2*(1+S))*da_a

Mlimit=np.zeros(2)

for i in range(N):
    n=3 #RELATIVISTIC CASE
    den0=K(n)**(-3/4)*c**(-2)*p0_r**(3/4) #central densities (
    polytrope)
    Rad_r[i,0]=1/2*(3*pi)**(1/2)*ksi1_r*(h_**(3/2)/(c**(1/2)*G
    **(1/2)*me*mN*A_Z))*(dencrit/den0[i])**(1/3)
    Rad_r[i,1]=Rad_r[i,0] * (1-y)
    M_r[i,0]=1/2*(3*pi)**(1/2)*ksi1_theta_r*(h_*c/G)**(3/2)*(mN*
    A_Z)**(-2)
    M_r[i,1]=M_r[i,0] * (1-y)
    Mlimit[0]=M_r[0,0]/Msun
    Mlimit[1]=M_r[0,1]/Msun
    Mdiff=abs(Mlimit[0]-Mlimit[1])

    n=3/2 #NON RELATIVISTIC CASE
    den0=K(n)**(-3/5)*c**(-2)*p0_n**(3/5)
    Rad_n[i,0]=((n+1)*K(n)*den0[i]**((1-n)/n)/(4*pi*G))**(1/2)*c
    **((n+1)/n)*ksi1_n
    Rad_n[i,1]=Rad_n[i,0] * (1-x)
    M_n[i,0]=4*pi*c**((3*n+3)/n)*((n+1)*K(n)/(4*pi*G))**(3/2)*den0
    [i]**((3-n)/(2*n))*ksi1_theta_n
    M_n[i,1]=M_n[i,0] * (1-x)

    Q=4*pi*c**((2*n+2)/(n-1))*((n+1)*K(n)/(4*pi*G))**(n/(n-1))*
    ksi1_n**((n-3)/(1-n))*ksi1_theta_n
    RM[i,0]=(M[i]/Q)**((1-n)/(3-n))
    RM[i,1]=RM[i,0] * (1-x)


#RELATIVISTIC CASE
fig, ax1 = plt.subplots()
plt.title('Relativistic White Dwarf')
color = 'tab:red'
ax1.set_xlabel('Central pressure (dyne/cm^2)')
```

```
plt.xscale('log')

ax1.set_ylabel('R (km)', color=color)
ax1.plot(p0_r*Pa2dyne_cm2,Rad_r[:,0]*1e-3,color=color, label='
    Radius')
ax1.tick_params(axis='y', labelcolor=color)
# ax1.set_ylim(bottom=2000, top=16000)

# Creating a twin Axes for the mass on the right y-axis
ax2=ax1.twinx()
color = 'tab:blue'
ax2.set_ylabel('Perturbed R (km)', color=color)
ax2.plot(p0_r*Pa2dyne_cm2,Rad_r[:,1]*1e-3,color=color, label='
    Radius with Couplings')
ax2.tick_params(axis='y', labelcolor=color)
# ax2.set_ylim(bottom=2000, top=16000)
plt.show()


fig, ax1 = plt.subplots()
plt.title('Relativistic White Dwarf')
color='tab:red'
ax1.set_xlabel('Central pressure (dyne/cm^2)')
plt.xscale('log')

ax1.set_ylabel('M (Mo)',color=color)
ax1.plot(p0_r*Pa2dyne_cm2,M_r[:,0]/Msun,color=color,label='Mass')
ax1.tick_params(axis='y',labelcolor=color)
# ax1.set_ylim(bottom=1.17, top=1.45)

#Creating a twin Axes for the mass on the right y-axis
ax2=ax1.twinx()
color='tab:blue'
ax2.set_ylabel('Perturbed M (Solar Masses)',color=color)
ax2.plot(p0_r*Pa2dyne_cm2,M_r[:,1]/Msun,color=color,label='Mass
    with Couplings')
ax2.tick_params(axis='y',labelcolor=color)
# ax2.set_ylim(bottom=1.17, top=1.45)
plt.show()


####################
#NON RELATIVISTIC CASE
fig, ax1 = plt.subplots()
plt.title('Non Relativistic White Dwarf')
color = 'tab:red'
ax1.set_xlabel('Central pressure (dyne/cm^2)')
# plt.xscale('log')

ax1.set_ylabel('R (km)', color=color)
```

```
221 ax1.plot(p0_n*Pa2dyne_cm2,Rad_n[:,0]*1e-3,color=color, label='
    Radius')
222 ax1.tick_params(axis='y', labelcolor=color)
223 # ax1.set_ylim(bottom=9000, top=16000)
224
225 # Creating a twin Axes for the mass on the right y-axis
226 ax2=ax1.twinx()
227 color = 'tab:blue'
228 ax2.set_ylabel('Perturbed R (km)', color=color)
229 ax2.plot(p0_n*Pa2dyne_cm2,Rad_n[:,1]*1e-3,color=color, label='
    Radius with Couplings')
230 ax2.tick_params(axis='y', labelcolor=color)
231 # ax2.set_ylim(bottom=9000, top=16000)
232 plt.show()
233
234
235 fig, ax1 = plt.subplots()
236 plt.title('Non Relativistic White Dwarf')
237 color='tab:red'
238 ax1.set_xlabel('Central pressure (dyne/cm^2)')
239 # plt.xscale('log')
240
241 ax1.set_ylabel('M (Solar Masses)',color=color)
242 ax1.plot(p0_n*Pa2dyne_cm2,M_n[:,0]/Msun,color=color,label='Mass')
243 ax1.tick_params(axis='y',labelcolor=color)
244 # ax1.set_ylim(bottom=0.15,top=0.55)
245
246
247 #Creating a twin Axes for the mass on the right y-axis
248 ax2=ax1.twinx()
249 color='tab:blue'
250 ax2.set_ylabel('Perturbed M (Solar Masses)',color=color)
251 ax2.plot(p0_n*Pa2dyne_cm2,M_n[:,1]/Msun,color=color,label='Mass
    with Couplings')
252 ax2.tick_params(axis='y',labelcolor=color)
253 # ax2.set_ylim(bottom=0.15,top=0.55)
254 plt.show()
255
256 ####################
257 # MASS RADIUS RELATION
258 maxR=max([max(RM[:,0]), max(RM[:,1])])
259 minR=min([min(RM[:,0]), min(RM[:,1])])
260 fig, ax1 = plt.subplots()
261 plt.title('Non Relativistic White Dwarf')
262 color = 'tab:red'
263 ax1.set_xlabel('M (Solar Masses)')
264 # plt.xscale('log')
265
266 ax1.set_ylabel('R (km)', color=color)
267 ax1.plot(M/Msun,RM[:, 0]*1e-3,color=color, label='Radius')
268 ax1.tick_params(axis='y', labelcolor=color)
```

```
ax1.set_ylim(bottom=minR*1e-3, top=maxR*1e-3)

# Creating a twin Axes for the mass on the right y-axis
ax2=ax1.twinx()
color = 'tab:blue'
ax2.set_ylabel('Perturbed R (km)', color=color)
ax2.plot(M/Msun,RM[:, 1]*1e-3,color=color, label='Radius with
    Couplings')
ax2.tick_params(axis='y', labelcolor=color)
ax2.set_ylim(bottom=minR*1e-3, top=maxR*1e-3)
plt.show()

####################
# TOV WITH COUPLINGS
R=110 # change these parameters in the begining of the script (TOV
     function)
S=0
da_a=0.001
Mlimit=np.zeros([2]) # Chandrasekhar limit for both cases
def TOV_couplings(r,p_m,g):
    p,m=p_m #everything in SI
    if g==5/3:
        K=h_**2./(15.*pi**2.*me)*(3.*pi**2./(mN*c**2.*A_Z))
    **(5./3.)
        x=(0.8*R+0.5*(1+S))*da_a
    elif g==4/3:
        K=h_*c/(12.*pi**2.)*(3.*pi**2./(mN*c**2.*A_Z))**(4./3.)
        x=(0.8*R+0.2*(1+S))*da_a
    e=(p/K)**(1/g)
    p_e=K*e**(g-1)
    dp_dr=-G*e*m/(c**2*r**2) * (1+p_e) * (1+4*pi*r**3*p/(m*c**2))
    * \
            (1-2*G*m/(c**2*r))**(-1)
    dm_dr=4*pi*r**2*e/c**2
    dp_dr_a=dp_dr*(1-x**2)
    dm_dr_a=dm_dr*(1+x)
    # print([dp_dr,dm_dr,r])
    return [dp_dr_a,dm_dr_a]
sol=solve_ivp(TOV_couplings,(rstart,rend),[initial_p,1e-10],method
    ='RK45',t_eval=r,rtol=1e-6,atol=1e-10,args=(g,))
pr_a,ma_a=sol.y
Mlimit[0]=max(ma)/Msun
Mlimit[1]=max(ma_a)/Msun
Mdiff=abs(Mlimit[0]-Mlimit[1])
mlimit=max([max(ma),max(ma_a)])

fig, ax1 = plt.subplots()

color = 'tab:blue'
ax1.set_xlabel('r (km)')
```

```
314 plt.title(f'R={R}, S={S}, $\\gamma$={gtxt}, $\\Delta\\alpha/\\
    alpha$={da_a}')
315 ax1.set_ylabel('Pressure (dyne/cm^2)', color=color)
316 ax1.plot(r*1e-3, pr*Pa2dyne_cm2, color=color, label='Pressure')
317 ax1.tick_params(axis='y', labelcolor=color)
318 ax1.set_ylim(bottom=0, top=initial_p*Pa2dyne_cm2+1e21)
319
320 # Creating a twin Axes for the mass on the right y-axis
321 ax2=ax1.twinx()
322 color='tab:red'
323 ax2.set_ylabel('Pressure perturbed (dyne/cm^2)',color=color)
324 ax2.plot(r*1e-3,pr_a*Pa2dyne_cm2,color=color,label='Pressure P')
325 ax2.tick_params(axis='y',labelcolor=color)
326 ax2.set_ylim(bottom=0, top=initial_p*Pa2dyne_cm2+1e21)
327 plt.show()
328
329 fig, ax1 = plt.subplots()
330
331 color = 'tab:blue'
332 ax1.set_xlabel('r (km)')
333 plt.title(f'R={R}, S={S}, $\\gamma$={gtxt}, $\\Delta\\alpha/\\
    alpha$={da_a}')
334 ax1.set_ylabel('Mass (Mo)', color=color)
335 ax1.plot(r*1e-3,ma/Msun,color=color,label='Mass')
336 ax1.tick_params(axis='y', labelcolor=color)
337 ax1.set_ylim(bottom=0, top=mlimit/Msun+0.1)
338
339 # Creating a twin Axes for the mass on the right y-axis
340 ax2=ax1.twinx()
341 color='tab:red'
342 ax2.set_ylabel('Mass perturbed (Mo)',color=color)
343 ax2.plot(r*1e-3,ma_a/Msun,color=color,label='Mass P')
344 ax2.tick_params(axis='y',labelcolor=color)
345 ax2.set_ylim(bottom=0, top=mlimit/Msun+0.1)
346 plt.show()
```

B

Neutron Star Code

```
# Assuming you have imported the TOV class earlier
# from tovsolver.tov import TOV

# Import necessary modules
import numpy as np
import matplotlib.pyplot as plt
from scipy.interpolate import interp1d

pi=np.pi
MeV_fm3_to_pa = 1.6021766e32
G  = 6.6730831e-11 #SI
c  = 2.99792458e8  #SI
Msolar=1.9891e30 #kg
# Load the EoS data from the file
eos = np.genfromtxt("SLY4.txt")

# Extract neutron number density and pressure arrays from EoS data
e_arr, p_arr = eos[:, 4]*MeV_fm3_to_pa, eos[:, 3]*MeV_fm3_to_pa  # Pa
plt.loglog(e_arr,p_arr,'.',markersize=1.5)
plt.xlabel("Energy density MeV")
plt.ylabel("Pressure MeV")



# # # Initialize TOV solver with neutron number density and pressure arrays
# tov_s = TOV(e_arr, p_arr, plot_eos=True, add_crust=False)

# m_arr = []
# R_arr = []

# dens_c=np.logspace(-4, 3, 350)
```

```
# # Adjust the range of central densities as needed
# for dens_c in np.logspace(-4, 3, 350):
#     # Solve the TOV equations for the current central density
#     R, M, prof = tov_s.solve(dens_c, rmax=10e5, dr=100)
#     # Append the resulting mass and radius to the lists
#     m_arr.append(M)
#     R_arr.append(R)


# plt.plot(R_arr, m_arr)

# plt.xlim(10,20)
# plt.ylim(0,2.3)

# plt.ylabel(r'${\rm M/M_\odot}$')
# plt.xlabel(r'${\rm R~(km)}$')
#
    ########################################################################


## TOV EQNS AND RK4 STEP
# def A(R,S,n,da_a): #Perturbation depending on the GUT model and the EoS
#     return (4/5*R+(17-3*n)/(10*(1+n))*(1+S))*da_a

def dp_dr(r, p, m, n, K, Rp, Sp, da_a):
    e = ((p / K)**(n / (n + 1)))
    p_e= K*e**((n+1)/n -1)
    A=(4/5*Rp+(17-3*n)/(10*(1+(n))*(1+Sp)))*da_a
    return -G*m*e/(c**2*r**2) *  (1+p_e*(1-A))  *  (1+4*pi*r**3*p/(m*c**2))  *  (1-2*G*m/(c**2*r))**(-1)  *  (1+A)

def dm_dr(r, p, n, K):
    e = ((p / K)**(n / (n + 1)))
    return 4 * pi * r**2 * e / c**2

def rk4_step(r, dr, p, m, K, n, Rp, Sp, da_a):
    """
    Perform one step of fourth-order Runge-Kutta method.
    """
    # print([p,n])
    k1 = dr * dp_dr(r, p, m, n, K, Rp, Sp, da_a)
    l1 = dr * dm_dr(r, p, n, K)
    k2 = dr * dp_dr(r + 0.5 * dr, p + 0.5 * k1, m + 0.5 * l1, n, K, Rp, Sp, da_a)
    l2 = dr * dm_dr(r + 0.5 * dr, p + 0.5 * k1, n, K)
    k3 = dr * dp_dr(r + 0.5 * dr, p + 0.5 * k2, m + 0.5 * l2, n, K, Rp, Sp, da_a)
    l3 = dr * dm_dr(r + 0.5 * dr, p + 0.5 * k2, n, K)
    k4 = dr * dp_dr(r + dr, p + k3, m + l3, n, K, Rp, Sp, da_a)
    l4 = dr * dm_dr(r + dr, p + k3, n, K)
```

```
    dp = (k1 + 2 * k2 + 2 * k3 + k4) / 6
    dm = (l1 + 2 * l2 + 2 * l3 + l4) / 6

    return dp, dm

def solve_tov(p_central, Keff, neff, Rp, Sp, da_a, rmax, rstart, dr):
    pr=[]
    rad=[]
    ma=[]
    r = rstart  # Starting radius in m
    p = p_central #Starting pressure in m
    m = 1e-2    # Starting mass at center in m
    for _ in np.linspace(0,rmax,int(rmax/dr)): # only number of iterations (not r values)
        # if p>=p_arr[160]: # Pa
        #     K=7e-65         #6e-56      #7e-65
        #     n=0.6
        # else:
        #     K=1.2e-12
        #     n=3.6
        K=float(Keff(p))
        n=float(neff(p))
        # K=1.211485341708745e-13
        # n=3
        dp, dm = rk4_step(r, dr, p, m, K, n, Rp, Sp, da_a) # in Pa and kg respectively

        # if r>=10000 and r<=12000:
        #     print([p,dp,m,dm,r])

        #Check for NaN values
        if np.isnan(p):
            # Handle NaN value (e.g., set a default value)
            # print("NaN encountered in p. Terminating computation.")
            break
        elif np.isnan(dp) or np.isnan(dm):
            # Handle NaN values (e.g., set default values or terminate)
            # print("NaN encountered in dp or dm. Terminating computation.")
            break
        elif r>=7000 and abs(dm/m)<=1e-6:
            # print("Mass derivative 5 orders of magnitude smaller than mass. Terminating computation.")
            break
        p += dp # Pa
        m += dm # kg
        r += dr # m
        pr.append(p) # Pa
```

```
        ma.append(m) # kg
        rad.append(r) # m

    fig, ax1 = plt.subplots()
    plt.title(f'Central p: {central_pressure} Pa')
    color = 'tab:blue'
    ax1.set_xlabel('r (m)')
    ax1.set_ylabel('Pressure (Pa)', color=color)
    ax1.plot(rad, pr, color=color, label='Pressure')
    ax1.tick_params(axis='y', labelcolor=color)

    # Creating a twin Axes for the mass on the right y-axis
    ax2=ax1.twinx()
    color='tab:red'
    ax2.set_ylabel('Mass (kg)',color=color)
    ax2.plot(rad,ma,color=color,label='Mass')
    ax2.tick_params(axis='y',labelcolor=color)

    return r, m

#
    ##############################################################################################

# CREATE ARRAYS FOR neff AND Keff + APPLICATION
#
n=[2, 7, 14, 28] #datapoints per step
neff=np.zeros((4,196))
Keff=np.zeros((4,196))
e=np.zeros((4,196))
K_int=[None]*4
n_int=[None]*4
for m in range(0,4):
    for i in range(0,195,n[m]):
        a = np.polyfit(np.log10(e_arr[i:i+n[m]]),np.log10(p_arr[i:
    i+n[m]]), 1)
        ne=1/(a[0]-1) #doesn't change with unit conversion (its a
    slope)
        K=10**a[1]   #in SI
        for j in range(0,n[m]):
            neff[m,i+j]=ne
            Keff[m,i+j]=K
    for i in range(0,196):
        e[m,i]=(p_arr[i]/Keff[m,i])**(neff[m,i]/(neff[m,i]+1))
        K_int[m] = interp1d(p_arr, Keff[m,:], kind='linear',
    bounds_error=False, fill_value='extrapolate')
        n_int[m] = interp1d(p_arr, neff[m,:], kind='linear',
    bounds_error=False, fill_value='extrapolate')
fig, axes = plt.subplots(nrows=2, ncols=2, figsize=(8, 6))
for i in range(0,4):
    row = i // 2
    col = i % 2
```

```
166     axes[row,col].loglog(e_arr,p_arr,'k.',markersize=1.1)      #SI
167     axes[row,col].loglog(e[i,:],p_arr,color=(3/255, 86/255,
    115/255, 0.9))
168     axes[row,col].text(e[i, :].mean()/1e3, p_arr.mean(), f"{n[i]}
    points per step", horizontalalignment='center')
169 axes[1,0].set_ylabel("Pressure (Pa)")
170 axes[1,0].set_xlabel("Energy Density (Pa)")
171 K_int=K_int[0]
172 n_int=n_int[0]
173
174 # #FOR A POLYTROPE
175 # MeV2kg=1.78266269594644e-30
176 # A_Z=2
177 # mp=938.27208816*MeV2kg # kg
178 # mn=939.5654205*MeV2kg # kg
179 # mN=(mp+mn)/2 # kg
180 # h=6.62607015e-34 # kg*m^2*s^(-1)
181 # h_=h/(2*pi)
182 # c=3.0e8 #m*s^(-1)
183 # K_int=[]
184 # n_int=[]
185 # for i in range(0,195):
186 #     K_int.append(h_*c/(12.*pi**2.)*(3.*pi**2./(mN*c**2.*A_Z))
    **(4./3.))
187 #     n_int.append(3)
188
189 #Example usage
190 N=1000
191 da_a=[1e-3, -1e-3]
192 S=[160, 0, 22.5]
193 R=[36, 109.4, -183]
194 Radius = np.zeros(N)
195 Mass = np.zeros(N)
196 Radius1 = np.zeros((2,N))
197 Mass1 = np.zeros((2,N))
198 Radius2 = np.zeros((2,N))
199 Mass2 = np.zeros((2,N))
200 Radius3 = np.zeros((2,N))
201 Mass3 = np.zeros((2,N))
202
203 central_pressures=np.linspace(p_arr[1],p_arr[195],N)
204 for m in range(1,4): #K_int, n_int for 4 discretizations
205     for j in range(0,N-1): #Mass-radius datapoints
206         central_pressure=central_pressures[j]
207         rmax=30e4 #m
208         rstart=1e-2 #m
209         dr=1 #m
210         for i in range(2): #da_a cases
211             radius, mass = solve_tov(central_pressure, K_int[m],
    n_int[m], 0, 0, 0, rmax, rstart, dr) # in m and kg
    respectively
```

```
            Radius[j]=radius*1e-3 # km
            Mass[j]=mass/Msolar   # Msolar
            radius, mass = solve_tov(central_pressure, K_int[m],
    n_int[m], R[0], S[0], da_a[i], rmax, rstart, dr) # in m and kg
     respectively
            Radius1[i,j]=radius*1e-3 # km
            Mass1[i,j]=mass/Msolar   # Msolar
            radius, mass = solve_tov(central_pressure, K_int[m],
    n_int[m], R[1], S[1], da_a[i], rmax, rstart, dr) # in m and kg
     respectively
            Radius2[i,j]=radius*1e-3 # km
            Mass2[i,j]=mass/Msolar   # Msolar
            radius, mass = solve_tov(central_pressure, K_int[m],
    n_int[m], R[2], S[2], da_a[i], rmax, rstart, dr) # in m and kg
     respectively
            Radius3[i,j]=radius*1e-3 # km
            Mass3[i,j]=mass/Msolar   # Msolar
    # print("Central Pressure:", central_pressure, 'Pa')
    # print("Radius:", radius, 'm')
    # print("Mass:", mass/Msolar, "Msun")

color = [(3/255, 86/255, 115/255, 0.9), (3/255, 86/255, 115/255,
    0.5)]
p=[r"10^{-3}", r"-10^{-3}"]
plt.figure()
plt.plot(Radius[1:9999],Mass[1:9999],'k', label=r"$d\alpha/\alpha
    =0$") # km and Msolar respectively
for i in range(2):
    plt.plot(Radius1[i,1:9999],Mass1[i,1:9999], color=color[i],
    label=r"$d\alpha/\alpha="+p[i]+"$") # km and Msolar
    respectively
plt.ylabel("Mass (Msolar)")
plt.xlabel("Radius (km)")
# plt.title("Unification")
plt.legend()
# plt.ylim([0, 1.4])
# plt.xlim([0, 15])

plt.figure()
plt.plot(Radius[1:9999],Mass[1:9999],'k', label=r"$d\alpha/\alpha
    =0$") # km and Msolar respectively
for i in range(2):
    plt.plot(Radius2[i,1:9999],Mass2[i,1:9999], color=color[i],
    label=r"$d\alpha/\alpha="+p[i]+"$") # km and Msolar
    respectively
plt.ylabel("Mass (Msolar)")
plt.xlabel("Radius (km)")
# plt.title("Dilaton")
plt.legend()
# # plt.ylim([0, 1.4])
# # plt.xlim([0, 15])
```

```
250
251 plt.figure()
252 plt.plot(Radius[1:9999],Mass[1:9999],'k', label=r"$d\alpha/\alpha
    =0$") # km and Msolar respectively
253 for i in range(2):
254     plt.plot(Radius3[i,1:9999],Mass3[i,1:9999], color=color[i],
    label=r"$d\alpha/\alpha="+p[i]+"$") # km and Msolar
    respectively
255 plt.ylabel("Mass (Msolar)")
256 plt.xlabel("Radius (km)")
257 # plt.title("UV cutoff")
258 # plt.legend()
259 # # plt.ylim([0, 1.4])
260 # # plt.xlim([0, 15])
```